Synthesis, Characterization, and Photochemistry of Novel Ru(II) Complexes for Light-Induced Enzyme Inhibition and Singlet Oxygen Generation

Undergraduate Research Thesis

Presented in partial fulfillment of the requirements for graduation with honors research distinction in Chemistry in the undergraduate colleges of The Ohio State University

by

Kelsey Collins

The Ohio State University

May 2016

Project Advisor: Professor Claudia Turro, Department of Chemistry and Biochemistry

Abstract

Photodynamic therapy (PDT) is a developing cancer treatment involving the use of a photoactive drug molecule that is inactive in the dark and activated by low energy light. A new pathway that is being explored is the caging of cytotoxic molecules by protecting groups that are photolabile. Divalent ruthenium complexes exhibit photoinduced ligand exchange, making these complexes prime candidates for investigation as new PDT agents. The synthesis and characterization by ^{1}H NMR of four ruthenium(II) complexes, [Ru(tpy)(NN)L]$(PF_6)_2$ where NN = bpy (bpy = 2,2′-bipyridine) or dppn (dppn = benzo[*i*]-dipyrido[3,2-*a*:2′,3′-*c*]phenazine) and L = CH_3CN or Cbz-Leu-$NHCH_2CN$, is reported. [Ru(tpy)(NN)Cbz-Leu-$NHCH_2CN$]$(PF_6)_2$ are proposed as potential PDT agents, as Cbz-Leu-$NHCH_2CN$ is a cathepsin K inhibitor capable of reducing or hindering tumor growth and metastasis. The photoinduced ligand exchange of all four complexes in water upon irradiation with visible light was monitored by electronic absorption spectroscopy. Complexes with a dppn ligand required longer irradiation times than complexes with a bpy ligand. The production of singlet oxygen in $[Ru(tpy)(dppn)(CH_3CN)]^{2+}$ was tracked with emission spectroscopy and the use of an emissive singlet oxygen scavenger, DPBF = 1,3-diphenylisobenzofuran, and the quantum yield is reported, $\Phi_\Delta = 0.62(6)$.

Introduction

The anticancer agent, cisplatin, *cis*-$[Pt(NH_3)Cl_2]$, and its derivatives have proved effective treatments for a variety of cancers.[1-6] Cisplatin is activated upon entering the cell and exchanging the two chloride ligands for water molecules. In this form, cisplatin is able to bind to the bases of DNA, and inhibit cell proliferation and effect cell death. The process of ligand exchange between the chloride and water ligands is activated thermally, and thus makes the drug

effective at targeting rapidly reproducing cells.[4-6] While this includes cancerous cells, cisplatin also targets healthy cells such as liver and hair cells, leading to a number of adverse effects.[5-6] Cisplatin is also selective to certain cancers but not others. Additionally, aggressive cancers, such as breast cancer, previously treated with a cisplatin-based treatment have also been shown to acquire a resistance to the drug. [1-6]

New treatment modalities are being explored to avoid the adverse effects associated with cisplatin based treatments. A current FDA-approved treatment is photodynamic therapy (PDT). PDT relies on the activation of drug molecules that are otherwise nontoxic by excitation with low energy visible light.[7-9] Low energy visible light (ca. 600-900 nm) is able to penetrate up to 2 cm of tissue, making it an ideal choice for activating drug molecules in membranes, cells, or in the vicinity of the tumor. This results in localized drug delivery centered on the cancerous region.

Current FDA-approved PDT agents are highly conjugated aromatic molecules that when irradiated with low energy visible are capable of producing singlet oxygen. When these molecules are irradiated, they are excited to a high energy singlet excited state and then relax to a lower energy long-lived triplet excited state.[10] Energy transfer from the triplet state to molecular oxygen results in the formation of singlet oxygen, which has been shown to be cytotoxic.[7, 11, 12] However, many aggressive, solid tumors are hypoxic in nature, limiting this mode of action.[10] To further the applications of PDT, new agents should be toxic independent of oxygen concentration and capable of efficiently absorbing the low energy visible light necessary for activation.

Ru(II) polypyridyl complexes have been shown to exhibit photoinduced ligand exchange.[13-16] Upon irradiation, the complex is excited to a high energy ^{1}MLCT (singlet metal-to-ligand charge transfer) state and rapidly undergoes intersystem conversion to the ^{3}MLCT (triplet metal-to-ligand charge transfer) state. From this state, the ^{3}LF (triplet ligand field) state is accessible and ligand dissociation is possible.[17] This ability of Ru(II) complexes make them prime candidates for PDT as they are capable of localized light-activated drug delivery of a bound drug molecule.

The drug molecule used is Cbz-Leu-$NHCH_2CN$, a cathepsin K enzyme inhibitor.[18] Cathepsin K has been shown to be overexpressed in bone marrow macrophages, osteoclasts, and breast cancer cells, and has been shown to promote tumor growth and metastasis. However, the enzyme is also important for function of healthy cells, such that inhibitors cannot be administered systemically to a patient. Therefore, the release of inhibitors in the vicinity of the tumor with light makes it a target for PDT.[18] Cbz-Leu-$NHCH_2CN$ is capable of binding to Ru(II) through the terminal nitrile (Figure 1), which prevents it from interacting with cathepsin K.[19] This makes Cbz-Leu-$NHCH_2CN$ a prime candidate for use in a PDT agent as it is nontoxic in the dark when bound to Ru(II) and can be exchanged with a water molecule upon visible light irradiation in an aqueous environment, thus releasing the inhibitor for therapeutic action.

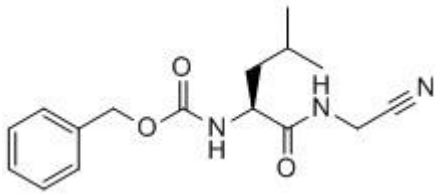

Figure 1: Chemical structure of Cbz-Leu-$NHCH_2CN$.

Ru(II) complexes are capable of dual action cytotoxicity.[17] If a singlet oxygen-producing ligand is coordinated to the metal center, the complex is able to produce singlet oxygen upon irradiation as well as release a bound therapeutic molecule. The ligand used for singlet oxygen production in the present work is dppn (benzo[*i*]-dipyrido[3,2-*a*:2′,3′-*c*]phenazine). When dppn is bound to Ru(II), the complex has a low-lying, long-lived $^3\pi\pi^*$ state capable of generating singlet oxygen with nearly 100% yield.[20]

The complexes under investigation are $[Ru(tpy)(bpy)(CH_3CN)]^{2+}$ (**1**; tpy = 2,2′:6′,2″-terpyridine, bpy = 2,2′-bipyridine,), $[Ru(tpy)(dppn)(CH_3CN)]^{2+}$ (**2**), $[Ru(tpy)(bpy)(Cbz\text{-}Leu\text{-}NHCH_2CN)]^{2+}$ (**3**) and $[Ru(tpy)(dppn)(Cbz\text{-}Leu\text{-}NHCH_2CN)]^{2+}$ (**4**), and their molecular structures are shown in Figure 2. The acetonitrile complexes **1** and **2** were investigated as controls for the corresponding drug-containing complexes **3** and **4**.

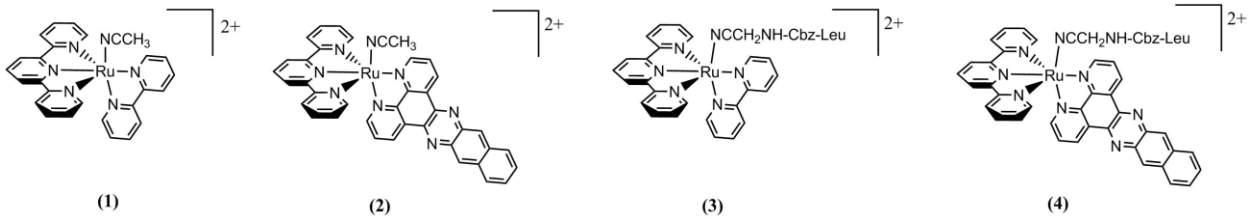

Figure 2: The proposed complexes for study: (1) $[Ru(tpy)(bpy)(CH_3CN)]^{2+}$, (2) $[Ru(tpy)(dppn)(CH_3CN)]^{2+}$, (3) $[Ru(tpy)(bpy)(Cbz\text{-}Leu\text{-}NHCH_2CN)]^{2+}$, and (4) $[Ru(tpy)(dppn)(Cbz\text{-}Leu\text{-}NHCH_2CN)]^{2+}$

Experimental Section

Materials

Standard Schlenk-line techniques were used to maintain anaerobic conditions during the preparation of compounds when necessary. The solvents used were of reagent grade quality. Water (ChromAR, Mallinckrodt, or deionized to 18 MOhm), 200 proof ethanol (Decon Laboratories), diethyl ether (Fisher Scientific), acetone (Fisher Scientific), methanol (Fisher Scientific), dichloromethane (Macron), hexanes (Macron) were used as received. Dimethylformamide (Sigma-Aldrich) was distilled to dryness. The reagents $RuCl_3 \cdot 3H_2O$ (Pressure Chemicals), 2,2′-bipyridine (Alfa Aesar), 2,2′:6′,2″-terpyridine (Sigma-Aldrich), lithium chloride (Sigma-Aldrich), triethylamine (Fisher Scientific), ammonium hexafluorate (Sigma-Aldrich), acetonitrile (Fisher Scientific), silver triflate (Sigma-Aldrich), silver tetrafluoroborate (Sigma-Aldrich), sodium bicarbonate (Fisher Scientific), potassium chloride (Sigma-Aldrich), Z-L-Leu-OH-DCA (Chem Impex), aminoacetonitrile hydrochloride (Pfaltz-Bauer), *O*-(Benzotriazol-1-yl)-*N,N,N′,N′*-tetramethyluronium hexafluorophosphate **(**HBTU) (Indofine), potassium ferrioxalate (Strem Chemicals), and 1,3-diphenylisobenzofuran (DPBF, Sigma-Aldrich) were purchased and used without further purification. Celite (Jenneile) was used as received. Neutral alumina (Fisher Scientific) was deactivated with methanol. Deuterated acetone (Sigma-Aldrich), chloroform (Sigma-Aldrich), and acetonitrile (Sigma-Aldrich) were used as received. The dppn ligand was prepared according to literature procedures.[20]

Synthesis of $Ru(tpy)Cl_3$

The synthesis of $Ru(tpy)Cl_3$ was adapted from a reported procedure.[21] A mixture of $RuCl_3 \cdot 3H_2O$ (560.5 mg, 2.14 mmol) and tpy (500.0 mg, 2.14 mmol) in 100 mL EtOH was heated at reflux for 4 hours. The reaction mixture was cooled to room temperature. The solid was collected by vacuum filtration and washed with EtOH (30 mL) and H_2O (15 mL).

Synthesis of [Ru(tpy)(bpy)Cl](PF$_6$)

Synthesis of $[Ru(tpy)(bpy)Cl](PF_6)$ was adapted from a reported procedure.[22] $Ru(tpy)Cl_3$ (100.5 mg, 0.228 mmol) was dissolved in 3:1 EtOH:H_2O (40 mL) with bpy (58 mg, 0.372 mmol), LiCl (90 mg, 2.12 mmol) and triethylamine (250 µL, 1.79 mmol) and heated at reflux for 4 hours. The reaction mixture was cooled to room temperature and stirred with excess NH_4PF_6. The solid was collected by vacuum filtration and washed with diethyl ether, and then dissolved in acetone and dried (yield = 41.4%).

Synthesis of [Ru(tpy)(dppn)Cl](PF$_6$)

$Ru(tpy)Cl_3$ (52.8 mg, 0.120 mmol), dppn (55.1 mg, 0.166 mmol), LiCl (45.0 mg, 1.06 mmol) and triethylamine (125 µL, 0.897 mmol) in 20 mL EtOH were heated at reflux for 4 hours. The reaction mixture was cooled to room temperature and stirred with NH_4PF_6. EtOH was removed with nitrogen, and the precipitate was collected by vacuum filtration and washed with H_2O, acetone, and toluene. Purification was achieved by dissolving the resulting solid in CH_2Cl_2 and centrifuging to remove solid. The complex was eluted from an alumina column with CH_2Cl_2 with 3% MeOH. A yellow band containing excess dppn eluted first, followed by a purple band containing the desired product.

Synthesis of $[Ru(tpy)(bpy)(CH_3CN)](PF_6)_2$

Synthesis of $[Ru(tpy)(bpy)(CH_3CN)](PF_6)_2$ was adapted from a reported procedure.[23] $[Ru(tpy)(bpy)Cl](PF_6)$ (31.3 mg, 0.0466 mmol) was dissolved and heated at reflux in a 20 mL 1:1 $CH_3CN:H_2O$ mixture overnight. The reaction mixture was cooled to room temperature and stirred with NH_4PF_6. The solid was collected by vacuum filtration. ^1H NMR ($(CD_3)_2CO$) δ 2.07 ppm (s, 3H), 7.04 (tq, 1H), 7.31 (m, 2H), 7.64 (dq, 2H), 7.77 (m, 1H), 7.94 (m, 3H), 8.29 (m, 4H), 8.37 (dq, 2H), 8.51 (d, 2H), 8.58 (d, 1H), 9.56 (dq, 1H).

Synthesis of $[Ru(tpy)(dppn)(CH_3CN)](PF_6)_2$

$[Ru(tpy)(dppn)Cl](PF_6)$ (33 mg, 0.0390 mmol) and $AgSO_3CF_3$ (9 mg, 0.0350 mmol) in 20 mL 1:1 $CH_3CN:H_2O$ were heated at reflux for 4 hours. The reaction was cooled to room temperature and stirred with NH_4PF_6. The solid was collected by vacuum filtration. ^1H NMR ($(CD_3)_2CO$) δ 2.43 ppm (s, 3H), 7.45 (m, 2H), 7.76 (m, 1H), 7.80 (m, 2H), 8.09 (d, 2H), 8.16 (m, 3H), 8.44 (m, 2H), 8.58 (t, 1H) 8.63 (q, 1H), 8.81 (dt, 2H) , 8.97 (dd, 2H), 9.15 (s, 1H), 9.25 (s, 1H). 9.52 (dd, 1H), 10.03 (dd, 1H), 10.35 (dd, 1H).

Synthesis of Cbz-Leu-$NHCH_2CN$

Cbz-Leu-$NHCH_2CN$ was synthesized according to a modified literature procedure.[24] Z-L-Leu-OH-DCA (1.8606 g, 446.6g/mol), aminoacetonitrile hydrochloride (0.7832 g) and HBTU (3.1435 g) in dry DMF (100 mL) were deoxygenated with nitrogen. Triethylamine (2.4 mL) was added and the reaction mixture was stirred at room temperature for 12 hours. The reaction mixture was filtered and CH_2Cl_2 (100 mL) was added to the yellow filtrate which was extracted with 0.1 M HCl (100 mL, 2 x), 1 M HCl (100 mL), saturated aqueous $NaHCO_3$ (100 mL), and

saturated aqueous KCl (100 mL). The organic fraction was collected and concentrated with nitrogen. The fraction was reprecipitated in hexanes, and the solid was collected by vacuum filtration and dried (yield = 57%). ^{1}H NMR (CD_3Cl) δ 0.81 ppm (3H, d), 0.85 (3H, d), 1.46 (1H, m), 1.54 (2H, m), 3.95 (2H, d), 4.17 (1H, m), 4.98 (2H, q), 5.45 (1H, d), 7.22 (5H, m), 7.34 (1H, m).

Synthesis of [Ru(tpy)(bpy)(Cbz-Leu-NHCH$_2$CN)](PF$_6$)$_2$

[Ru(tpy)(bpy)Cl](PF$_6$) (30 mg, 0.0447 mmol), Cbz-Leu-NHCH$_2$CN (40.6 mg, 0.134 mmol), and $AgBF_4$ (27.7 mg, 0.142 mmol) in 20 mL EtOH were heated at reflux overnight while shielded from light. The reaction mixture was cooled in an ice bath and filtered through celite and rinsed with EtOH. The reaction mixture was stirred with NH_4PF_6 and H_2O. Air was blown over the reaction mixture to remove EtOH while shielded from light. The solid was collected by vacuum filtration, and dissolved in acetone and centrifuged to remove excess ligand. The acetone solution was then reprecipitated in diethyl ether and collected by vacuum filtration. ^{1}H NMR ($(CD_3)_2CO$) δ 0.23 ppm (t, 2H), 0.40 (s, 2H), 0.58 (m, 2H), 0.73 (m, 2H), 2.68 (q, 1H), 3.16 (m, 1H), 3.32 (d, 1H), 3.38 (d, 1H), 4.14 (q, 2H), 5.73 (d, 1H) 6.36 (td, 1H), 6.46 (s, 5H), 6.62 (td, 3H), 6.76 (dt, 1H), 7.15 (m, 6H), 7.56 (m, 2H), 7.79 (t, 2H), 7.97 (d, 2H), 8.03 (d, 1H), 8.98 (d, 1H).

Synthesis of [Ru(tpy)(dppn)(Cbz-Leu-NHCH$_2$CN)](PF$_6$)$_2$

[Ru(tpy)(dppn)Cl](PF$_6$) (30 mg, 0.0354 mmol), Cbz-Leu-NHCH$_2$CN (107 mg, 0.353 mmol) and $AgBF_4$ (27.6 mg, 0.142 mmol) in 20 mL EtOH were deoxygenated with nitrogen and heated at reflux for 7 hours while shielded from light. The reaction mixture was cooled to room

temperature and filtered to remove impurities. The filtrate was a bright orange solution and was stirred with NH_4PF_6 and H_2O while nitrogen was blown over the filtrate to remove EtOH. The solid was collected by vacuum filtration and was dissolved in acetone. The solution was reprecipitated in diethyl ether and the solid was collected by vacuum filtration. ^{1}H NMR ($(CD_3)_2CO$) δ 1.25 ppm (s, 1H), 1.51 (m, 3H), 1.66 (m, 1H), 2.66 (m, 1H), 2.80 (m, 4H), 4.08 (m, 1H), 4.33 (d, 2H), 5.00 (dd, 2H), 6.62 (d, 1H), 7.30 (s, 5H), 7.40 (t, 2H), 7.68 (m, 3H), 7.97 (t, 1H), 8.01 (t, 2H), 8.07 (dd, 1H), 8.11 (t, 2H), 8.33 (m, 2H), 8.50 (t, 1H), 8.57 (dd, 1H), 8.72 (d, 2H), 8.88 (d, 2H), 9.04 (s, 1H), 9.13 (s, 1H), 9.40 (dd, 1H), 9.92 (dd, 1H), 10.28 (dd, 1H).

Instrumentation:

^{1}H NMR spectra were collected with a Bruker 250 MHz DPX spectrometer for bpy containing complexes and a Bruker 400 MHz DPX spectrometer for dppn containing complexes. Steady state absorption spectra were recorded on a Hewlett-Packard 8453 diode array spectrometer. Emission data for $^1O_2$ production quantum yields and room temperature and 77 K steady-state emission experiments were collected on a Horiba Fluoromax-4 spectrometer. Photolysis and ligand exchange quantum yield experiments were performed with a 150 W Xe arc lamp (USHIO) in a Miliarch lamp housing unit that was powered by an LPS-220 power supply equipped with an LPS-221 igniter (all from PTI). Bandpass filters (Thorlabs) and long pass filters (CVI Melles Griot) were used to select the appropriate excitation wavelengths.

Methods:

^{1}H NMR was performed in methanol-d_4 for [Ru(tpy)(bpy)Cl](PF_6), acetonitrile-d_3 for [Ru(tpy)(bpy)(CH_3CN)](PF_6)$_2$, dichloromethane-d_2 for [Ru(tpy)(dppn)Cl](PF_6), acetone-d_6 for

$[Ru(tpy)(dppn)(CH_3CN)](PF_6)_2$, $[Ru(tpy)(bpy)(CBZ\text{-}Leu\text{-}NHCH_2CN)](PF_6)_2$, and $[Ru(tpy)(dppn)(CBZ\text{-}Leu\text{-}NHCH_2CN)](PF_6)_2$.

Quantum yield of $^1O_2$ production was measured with $[Ru(bpy)_3]^{2+}$ as a standard ($\Phi = 0.81$)[25] and 1,3-diphenylisobenzofuran (DPBF) as a $^1O_2$ trap. Samples were measured in CH_3CN in a 1 × 1 cm quartz cuvette. The samples were absorption matched at the irradiation wavelength (A = 0.01 at 460 nm). The samples were irradiated in the presence of 1.0 μM DPBF and the decreased emission of DPBF was monitored as a function of time (λ_{exc} = 405 nm and λ_{em} = 479 nm). A plot of the emission intensity vs irradiation time provided a linear trend. The slope for $[Ru(tpy)(dppn)(CH_3CN)]^{2+}$ was compared to that of $[Ru(bpy)_3]^{2+}$ to afford the quantum yield.

Samples were measured in CH_3CN in a 1 x 1 cm quartz cuvette for room temperature experiments. Samples at 77 K were placed in an NMR tube in a quartz finger dewar containing liquid N_2. The dewar was mounted in the sample compartment of a Horiba Fluoromax-4 spectrometer. For both room temperature and 77 K emission experiments, samples were excited with λ_{exc} = 450 nm. For the excitation experiments, the emission was monitored at 600 nm at 77 K and 625 nm at room temperature. The emission and excitation signals were corrected for detector response.

The ligand exchange quantum yields were measured with an irradiation wavelength of 450 nm in H_2O with 10% acetone. Potassium tris(ferrioxalate) was used as the chemical actinometer to determine the photon flux of the lamp. [26]

Results and Discussion

Synthesis

The reaction scheme for the synthesis of $[Ru(tpy)(NN)(NCCH_3)](PF_6)_2$ is shown in Scheme 1. The first step involves the preparation of $Ru(tpy)Cl_3$ from $RuCl_3 \cdot 3H_2O$. The resulting $Ru(tpy)Cl_3$ complex was then reacted with the desired bidentate ligand, NN = bpy or dppn, to form the corresponding $[Ru(tpy)(NN)Cl](PF_6)$ complex. The final step involved the replacement of the chloride ligand with acetonitrile. The reaction scheme for the synthesis of $[Ru(tpy)(NN)(Cbz\text{-}Leu\text{-}NHCH_2CN)](PF_6)_2$ (NN = bpy, dppn) is shown in Scheme 1. The synthesis is similar to the synthesis for $[Ru(tpy)(NN)(NCCH_3)](PF_6)_2$, however in the last step the chloride ligand is replaced with the drug molecule. The schematic representation of the molecular structure of the complexes is shown in Figure 3.

Scheme 1: Synthesis of [Ru(tpy)(NN)(L)]2+ where NN = bpy or dppn and L = CH_3CN or Cbz-Leu-$NHCH_2CN$.

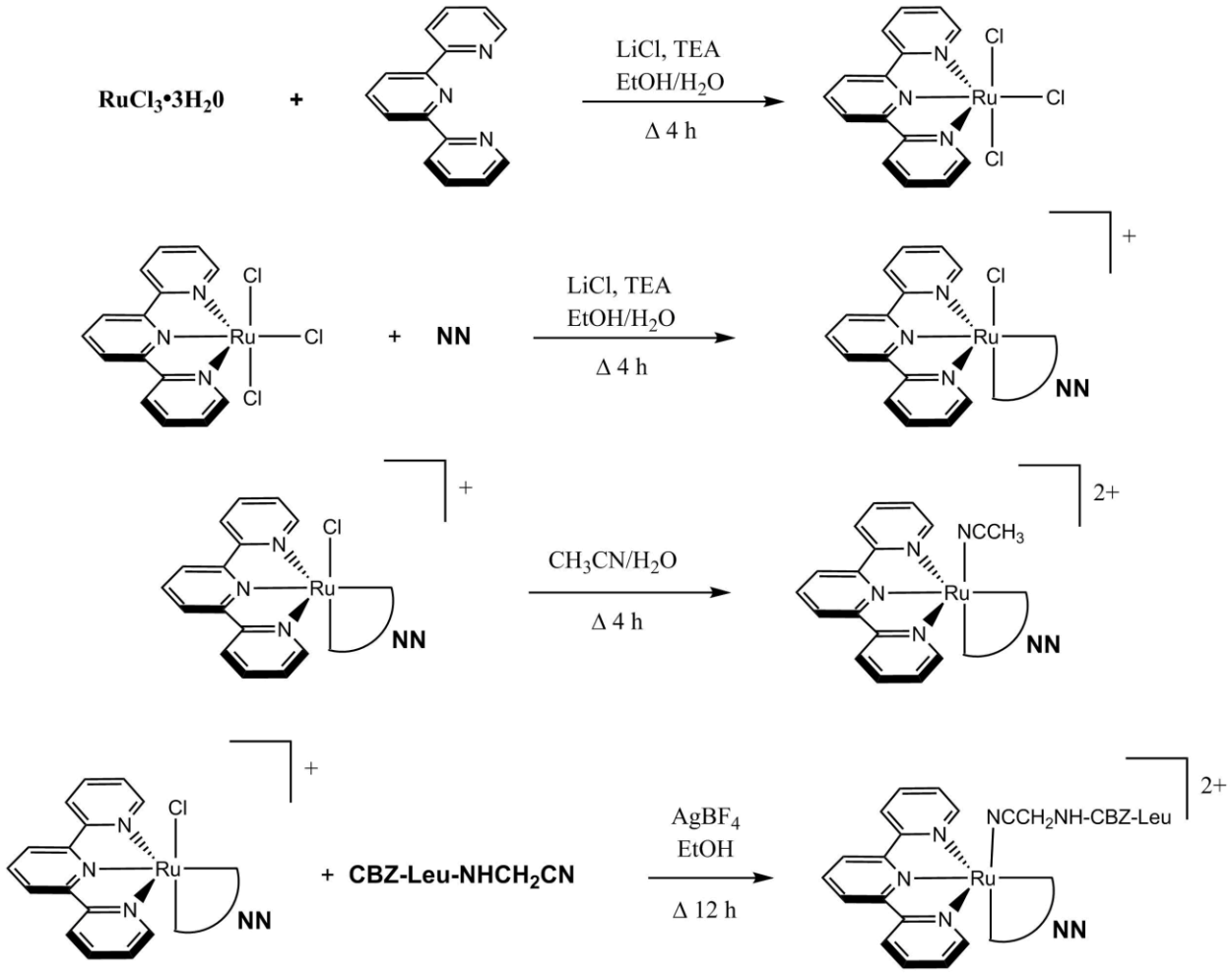

Structure

The ^{1}H-NMR spectra for $[Ru(tpy)(bpy)(CH_3CN)]^{2+}$ in $(CD_3)CO$ is shown in Figure 4 and the labeling scheme appears in Figure 3. A resonance integrating to 3H was observed at 2.07 ppm corresponding to the CH_3CN ligand bound to the ruthenium center (labeled c). The farthest downfield resonance in the spectrum was observed at 9.56 ppm and integrates to 1H, corresponding to the bpy proton pointing towards the acetonitrile ligand (labeled a). The ^{1}H-NMR spectra for $[Ru(tpy)(dppn)(CH_3CN)]^{2+}$ in $(CD_3)CO$ is shown in Figure 5. A resonance integrating to 3H was observed at 2.43 ppm corresponding to the CH_3CN ligand bound to the ruthenium center (labeled c). The farthest downfield resonance was observed at 10.35 ppm which integrates to 1H corresponding to the dppn proton pointing towards the acetonitrile ligand (labeled a). Two singlet resonances that both integrate to 1H were observed at 9.15 and 9.25 ppm (labeled b). These resonances correspond to the protons on the dppn backbone.

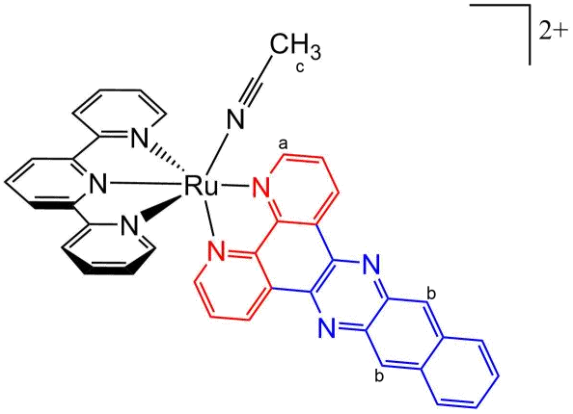

Figure 3: Structure of $[Ru(tpy)(NN)CH_3CN]^{2+}$ where the structure of the bpy ligand is shown in red, and the dppn ligand is comprised of both the red and blue structures. Small letters indicate proton assignments for the ^{1}H-NMR spectra below.

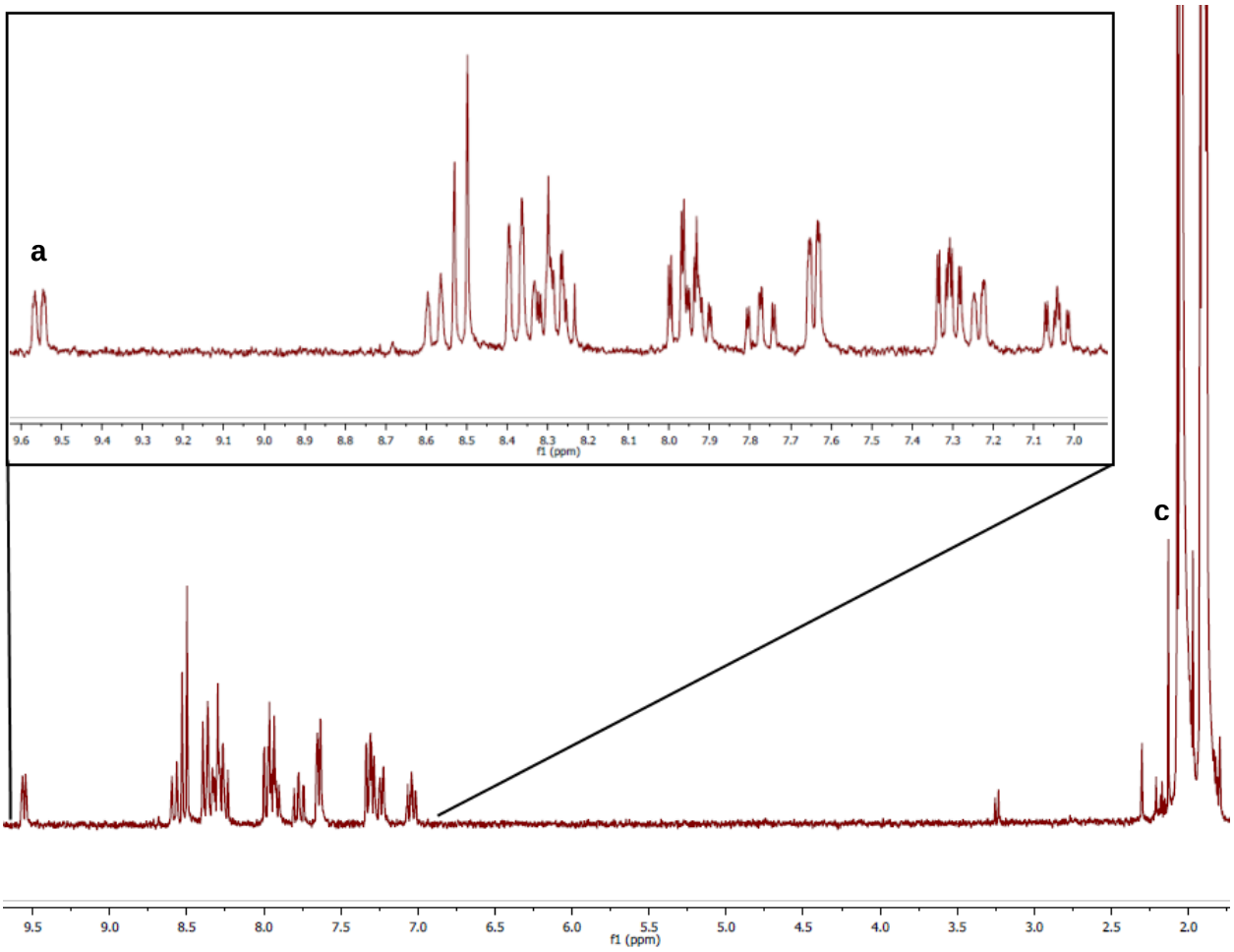

Figure 4: ^{1}H NMR spectra of $[Ru(tpy)(bpy)(CH_3CN)]^{2+}$

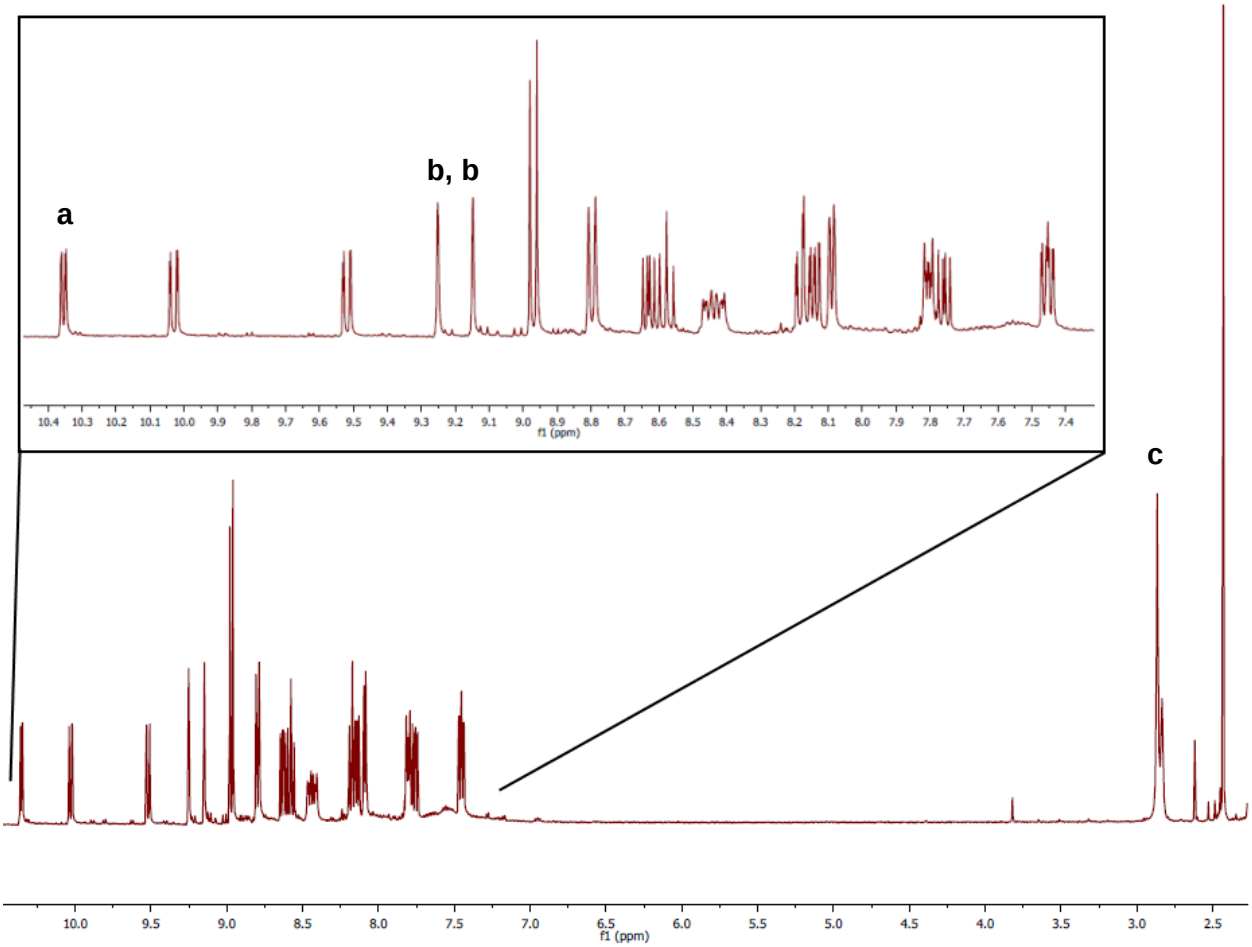

Figure 5: ^{1}H NMR spectra of $[Ru(tpy)(dppn)(CH_3CN)]^{2+}$

The molecular structure of $[Ru(tpy)(bpy)(CBZ\text{-}Leu\text{-}NHCH_2CN]^{2+}$ is depicted in Figure 6 (with proton labeling scheme) and its ^{1}H NMR spectrum in $(CD_3)CO$ is shown in Figure 7. A resonance integrating to 5H was observed at 6.46 ppm corresponding to the 5 protons of the phenyl ring in the inhibitor (labeled c). The farthest downfield resonance in the spectrum was observed at 8.98 ppm which integrates to 1H and corresponds to the bpy proton pointing towards the inhibitor (labeled a). This resonance has shifted between the acetonitrile and inhibitor complexes as the inhibitor is less electron withdrawing allowing the proton to be more shielded.

The ^{1}H-NMR spectra for $[Ru(tpy)(dppn)(CBZ\text{-}Leu\text{-}NHCH_2CN)]^{2+}$ in $(CD_3)CO$ is shown in Figure 8 and the structure of the molecule in Figure 6. A resonance integrating to 5H was observed at 7.30 ppm corresponding to the 5 phenyl protons of the inhibitor (c). The farthest downfield resonance was observed at 10.28 ppm integrating to 1H corresponds to the dppn proton pointing towards the inhibitor (a). Two singlet resonances that both integrate to 1H were observed at 9.04 and 9.13 ppm and corresponding to the dppn backbone protons (b).

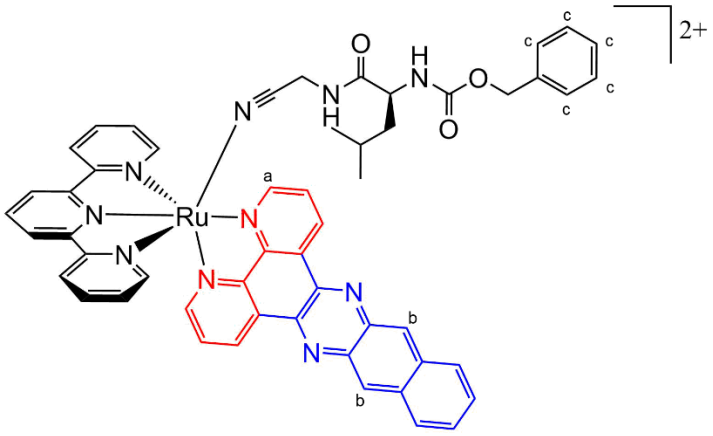

Figure 6: Structure of $[Ru(tpy)(NN)(Cbz\text{-}Leu\text{-}NHCH_2CN]^2$ where the structure of the bpy ligand is shown in red, and the dppn ligand is comprised of both the red and blue structures. Small letters indicate proton assignments for the ^{1}H-NMR spectra below.

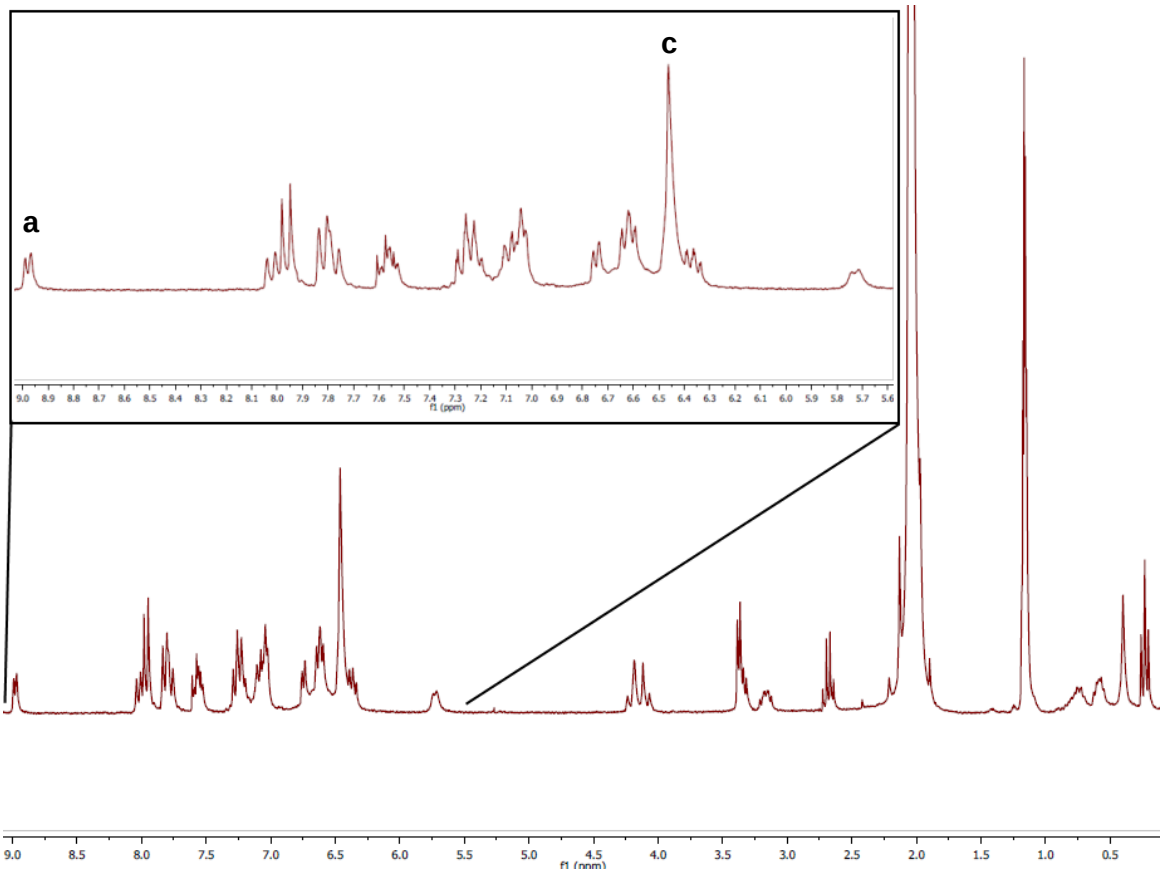

Figure 7: ^{1}H NMR of $[Ru(tpy)(bpy)(Cbz\text{-}Leu\text{-}NHCH_2CN)]^{2+}$

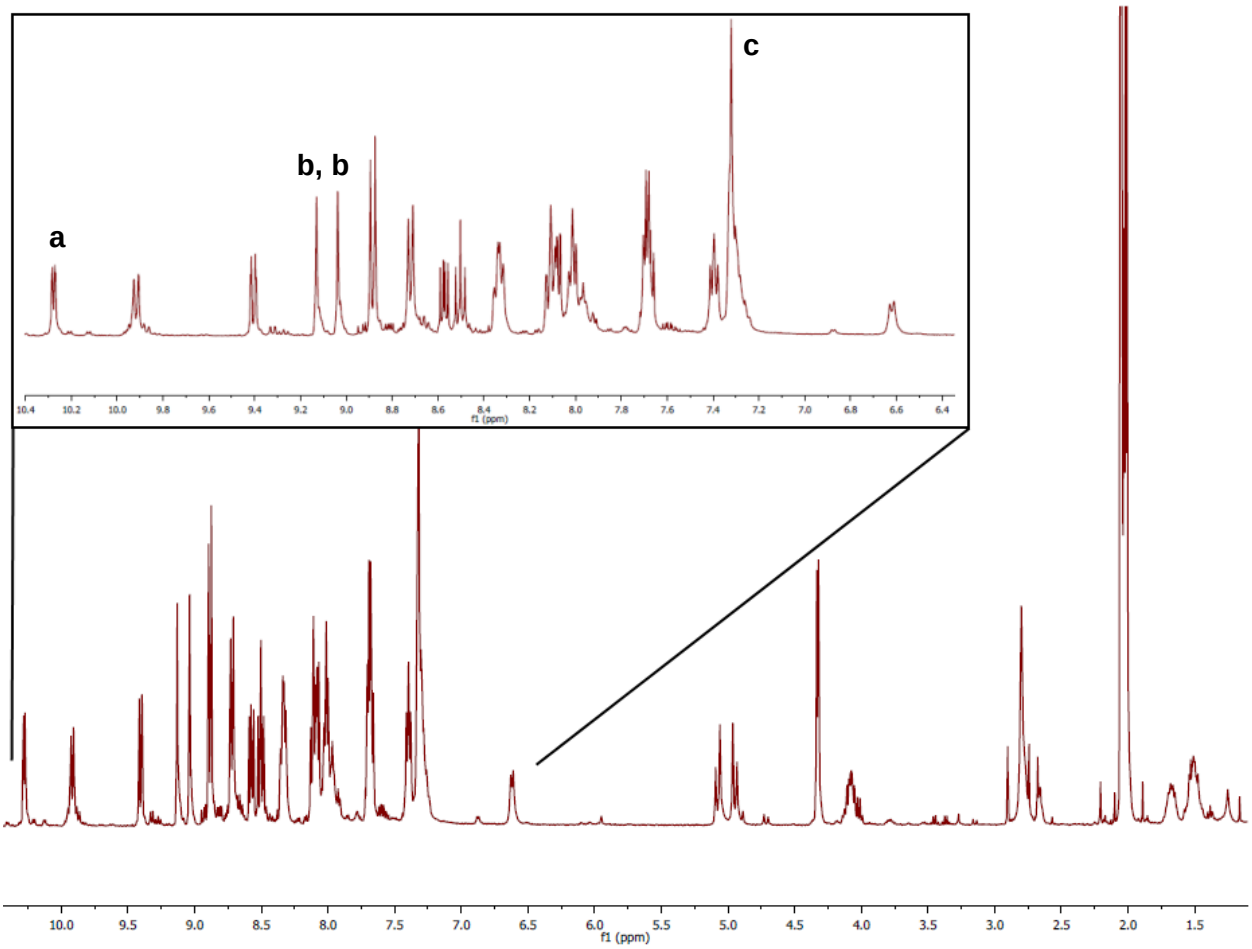

Figure 8: ^{1}H NMR of $[Ru(tpy)(dppn)(Cbz\text{-}Leu\text{-}NHCH_2CN)]^{2+}$

The electronic absorption spectrum of each complex in acetone exhibits a maximum at ~455 nm (Table 1), corresponding to the Ru→tpy and Ru→bpy/dppn metal-to-ligand charge transfer (^{1}MLCT) transitions. The bpy and dppn containing complexes have similar MLCT energies, indicating the proximal orbitals of dppn are not communicating electronically with the distal orbitals. In the dppn complexes, there are also maxima at 388 nm and 410 nm known to arise from ligand-centered $^{1}\pi\pi^{*}$ transitions of dppn (Table 1).

Table 1. Maxima Observed in the Electronic Absorption Spectrum of Each Complex in Water with 10% Acetone.

Complex	^{1}MLCT (λ / nm)	$^1\pi\pi^*$ (λ / nm)
$[Ru(tpy)(bpy)(CH_3CN)]^{2+}$	454	-
$[Ru(tpy)(bpy)(CBZ\text{-}Leu\text{-}NHCH_2CN)]^{2+}$	449	-
$[Ru(tpy)(dppn)(CH_3CN)]^{2+}$	452	388, 410
$[Ru(tpy)(dppn)(CBZ\text{-}Leu\text{-}NHCH_2CN)]^{2+}$	448	389, 410

A solution of each acetonitrile complex in acetonitrile was excited with λ_{ex} = 450 nm at 77 K. Both complexes exhibit emission with a peak near 600 nm (Table 2) consistent with the triplet metal-to-ligand charge transfer (^{3}MLCT) transition (Figure 9). There is a shoulder in the emission band near 650 nm (Table 2), corresponding to an energy difference between the peak and shoulder of 1150 cm^{-1} (Table 2). This energy difference corresponds to the energy difference in the vibrational levels of the ground state of each complex, as emission occurs from the lowest vibrational state of the ^{3}MLCT to discrete vibrational levels of the ground state. At low temperatures, the difference in energy between these transitions is resolved enough to be visible.

The complexes are very weakly emissive at room temperature (Figure 10), and the emission maxima for both complexes is red shifted compared to those at 77 K (Table 2). While emission is still occurring from the lowest possible energy vibrational level in the ^{3}MLCT state, relaxation is occurring to higher vibrational levels in the ground state, leading to lower energy phosphorescence. A clear shoulder in the emission spectrum is no longer visible, as more vibrational levels are accessible at higher temperatures, and the emission peak is broadened. The excitation spectra of the complexes (Figures 9 and 10, shown in gray) match the absorption

spectra, indicating the emission is occurring from the complexes and does not originate from an emissive impurity.

Table 2: Peaks in emission spectra of acetonitrile complexes in acetonitrile at 77K and room temperature.

Complex	λ_{max} - 77 K	$\lambda_{shoulder}$ - 77 K	ΔE (max, shoulder)	λ_{max} - RT, under N_2
$[Ru(tpy)(bpy)(CH_3CN)]^{2+}$	608 nm	653 nm	1133 cm^{-1}	624 nm
$[Ru(tpy)(dppn)(CH_3CN)]^{2+}$	598 nm	643 nm	1170 cm^{-1}	625 nm

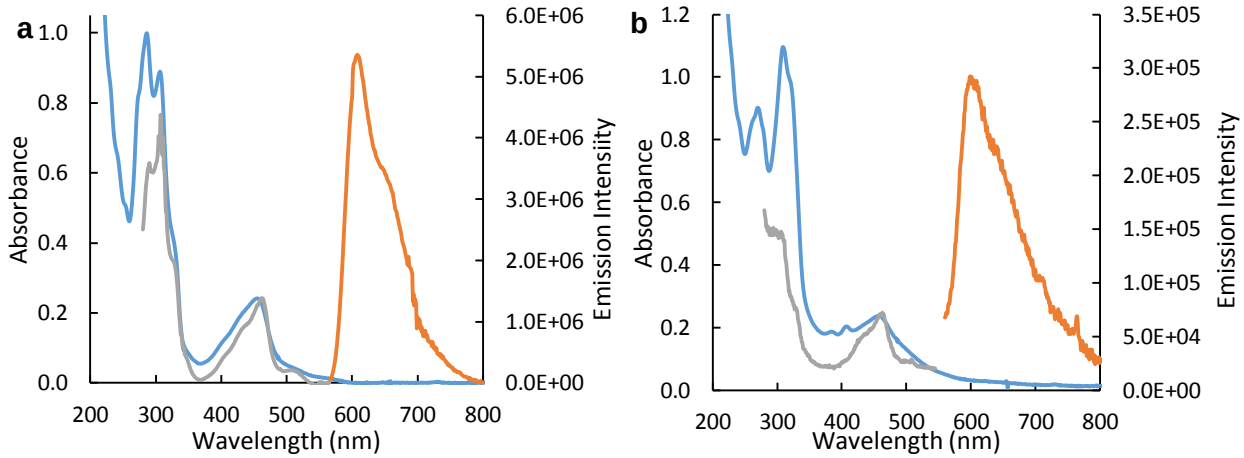

Figure 9 Absorption (blue, 298 K), excitation (grey, 77 K), and emission (orange, 77 K) spectra of (a) $[Ru(tpy)(bpy)(CH_3CN)]^{2+}$ and (b) $[Ru(tpy)(dppn)(CH_3CN)]^{2+}$ in acetonitrile.

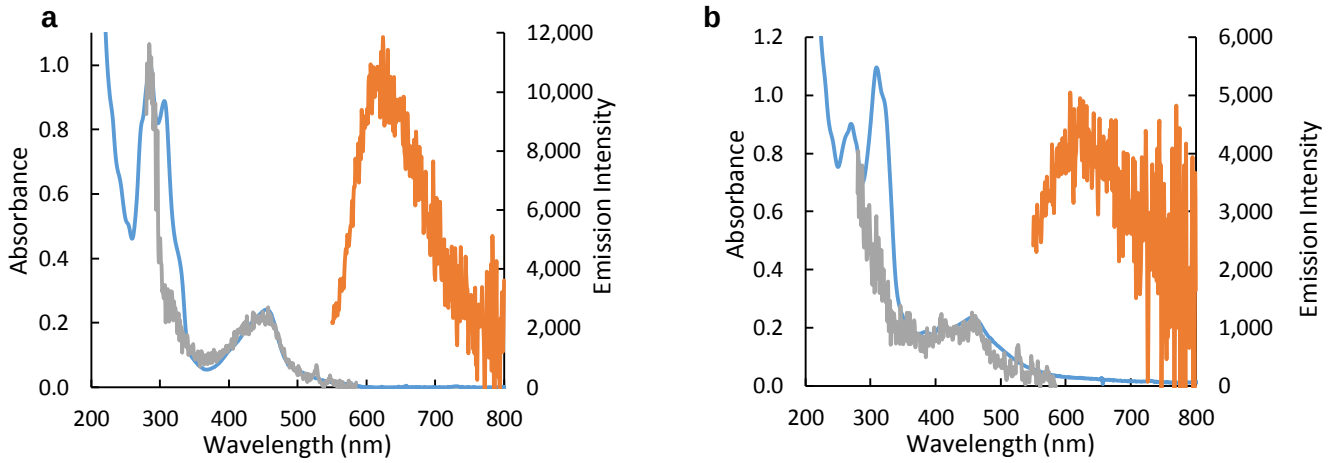

Figure 10: Absorbance (blue), excitation (grey), and emission (orange) spectra of $[Ru(tpy)(bpy)(CH_3CN)]^{2+}$ (a) and $[Ru(tpy)(dppn)(CH_3CN)]^{2+}$ (b) in acetonitrile at room temperature under nitrogen.

Irradiation into the ^{1}MLCT band of each complex with $\lambda_{irr} \geq 395$ nm results in ligand exchange in water (10% acetone). For the bpy containing complexes a decrease in the absorption at 455 nm was observed and a peak at 475 nm grew in (Figure 11, 13). These changes correspond to the release of a nitrile ligand and the coordination of a water molecule to form the photoproduct $[Ru(tpy)(bpy)(H_2O)]^{2+}$. The isosbestic points at 378 nm and 463 nm indicate the formation of a single photoproduct. For the dppn containing complexes a decrease in the absorption at 455 nm and an increase in absorption at 476 nm was observed, corresponding to the release of the nitrile ligand and the coordination of a water molecule to form the photoproduct $[Ru(tpy)(dppn)(H_2O)]^{2+}$ (Figure 12, 14). There was also decreased absorption on the ligand centered transition peaks at 388 and 410 nm, which was observed both in air and under nitrogen. The isosbestic point at 462 nm indicates the formation of a single photoproduct.

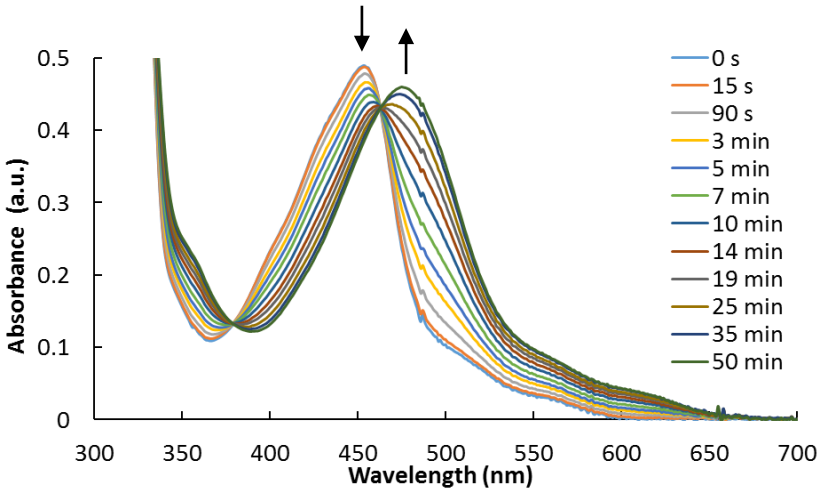

Figure 10: Photolysis of $[Ru(tpy)(bpy)(CH_3CN)]^{2+}$ in water.

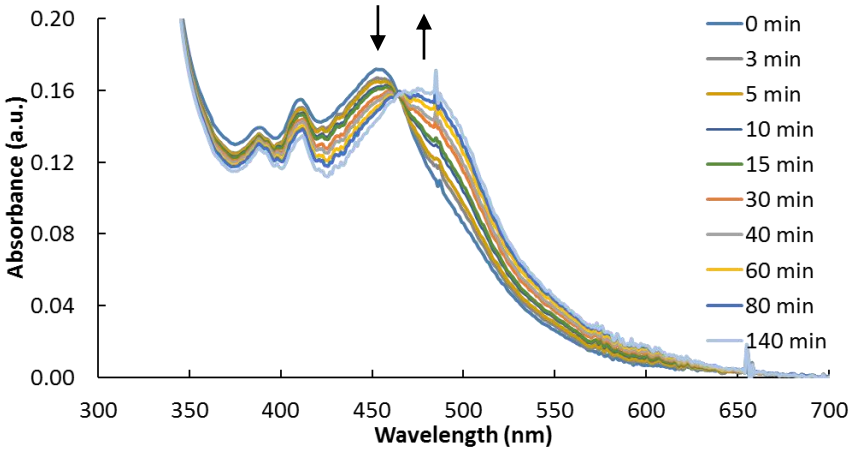

Figure 11: Photolysis of $[Ru(tpy)(dppn)(CH_3CN)]^{2+}$ in water.

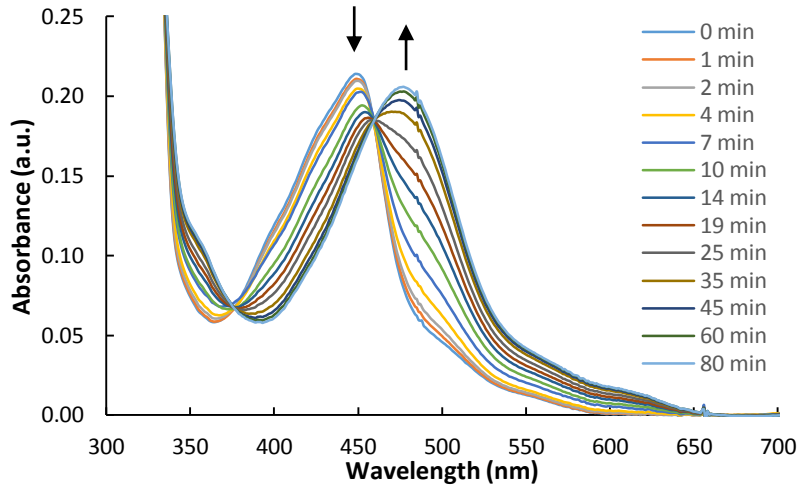

Figure 12: Photolysis of [Ru(tpy)(bpy)(CBZ-Leu-NHCH$_2$CN)]$^{2+}$

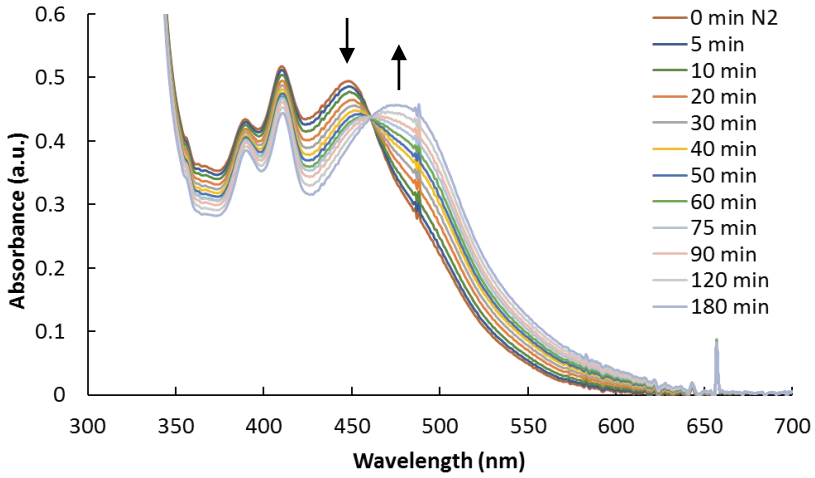

Figure 134: Photolysis of [Ru(tpy)(dppn)(CBZ-Leu-NHCH$_2$CN)]$^{2+}$

The drug containing complexes required longer irradiation times for conversion to the aqua complex than the acetonitrile complexes. This can be explained due to the size of the drug molecule. Since the drug is much larger than acetonitrile, it will diffuse in solution more slowly, allowing the drug to re-coordinate after its initial release, instead of being exchanged with a water molecule. The solubility of Cbz-Leu-NHCH$_2$CN in water is also lower than that of

CH_3CN, which also slows the diffusion of the dissociated ligand away from the metal complex, thus lowering the ligand exchange efficiency relative to the CH_3CN analogue.

The dppn containing complexes also required longer irradiation times than the bpy containing complexes as dppn is capable of generating $^1O_2$ from its long-lived $^3\pi\pi^*$ state. The processes of ligand exchange and singlet oxygen production are competitive as they arise from two different excited states that may be populated from the ^{1}MLCT excited state, making each process less efficient than in a complex where only one process is possible.[27]

$[Ru(tpy)(dppn)(CH_3CN)]^{2+}$ is capable of photoinduced ligand exchange as well as production of $^1O_2$ for enhanced cellular toxicity. The decrease in emission from the emissive $^1O_2$ scavenger, DPBF, in solution with $[Ru(tpy)(dppn)(CH_3CN)]^{2+}$ (orange) and $[Ru(bpy)_3]^{2+}$ (blue) is shown in Figure 15. The quantum yield of $^1O_2$ production (Φ_Δ) from the $^3\pi\pi^*$ state of $[Ru(tpy)(dppn)(CH_3CN)]^{2+}$ was determined to be 0.62(6). This value is lower than the quantum yield of $^1O_2$ production of $[Ru(bpy)_3]^{2+}$ (Φ_Δ = 0.81), which was used as a standard, due to the competition between the ^{3}LF responsible for ligand dissociation and $^3\pi\pi^*$ states responsible for the production of $^1O_2$.

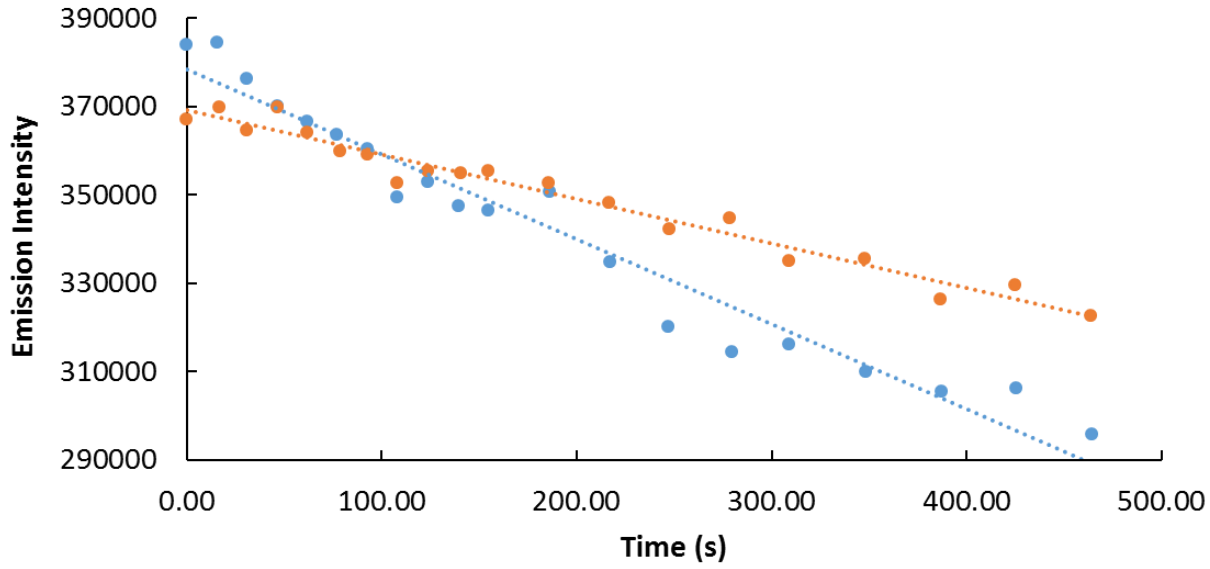

Figure 14: The emission of DPBF as a function of time while being irradiated in solution with a Ru(II) $^1O_2$ producer. $[Ru(bpy)_3]^{2+}$ is shown in blue, $[Ru(tpy)(dppn)(CH_3CN)]^{2+}$ is shown in orange.

Conclusion

$[Ru(tpy)(bpy)(CH_3CN)]^{2+}$ and $[Ru(tpy)(dppn)(CH_3CN)]^{2+}$ were synthesized as models for the potential PDT agents, $[Ru(tpy)(bpy)(Cbz\text{-}Leu\text{-}NHCH_2CN)]^{2+}$ and $[Ru(tpy)(dppn)(Cbz\text{-}Leu\text{-}NHCH_2CN)]^{2+}$, which were also synthesized and characterized. All four complexes are shown to undergo efficient photoinduced ligand exchange in an aqueous environment, and $[Ru(tpy)(dppn)(CH_3CN)]^{2+}$ was shown to efficiently produce singlet oxygen, enhancing the proposed cytotoxicity for $[Ru(tpy)(dppn)(Cbz\text{-}Leu\text{-}NHCH_2CN)]^{2+}$.

Acknowledgements

I would like to thank my thesis advisor, Professor Claudia Turro, and project mentor, Dr. Jessica White, for their support and guidance in this project. I would also like to thank my fellow Turro group members, specifically T.J. Rohrbaugh, Lauren Loftus, and Tyler Whittemore for their assistance in experiments and synthesis that was invaluable in completing this project. I am also grateful for Professor Terry Gustafson for encouraging me to participate in research in the first place.

References

[1] Oliver, T.; Mead, T. *Curr. Opin. Oncol*. 5 (**1993**) 559–567.

[2] Statopoulous, G.; Rigatos, S.; Melamos, N. A. *Oncol. Rep*. 6 (**1999**) 797 – 800.

[3] Bruhn, S.L.; Toney, J.H.; Lippard, S.J. *Prog. Inorg. Chem*. 38 (**1990**) 477 – 516.

[4] Kellard, L. R.; Farrell, N. P. *Platinum-based Drugs in Cancer Therapy*, Humana Press, N. J., 2000.

[5] Masters, J. R.; Köberle, B. *Nat. Rev. Cancer* 3 **(2003**) 517 – 525.

[6] Jung, Y.; Lippard, S. J. *J. Chem. Rev.* 107 (**2007**) 1387 – 1407.

[7] Juzeniene, A.; Peng, Q.; Moan, J. *Photochem. Photobiol. Sci*. 6 (**2007**) 1234 – 1245. 25

[8] DeRosa, M. C.; Crutchley, R. J. *Coord. Chem. Rev.* 233 – 234 (**2002**) 351 – 371. 26

[9] Detty, M. R.; Gibson, S. L.; Wagner, S.J. *J. Med. Chem.* 47 (**2004**) 3897 – 3915. 27

[10] Sears, R. B.; Joyce, L. E.; Ojaimi, M.; Gallucci, J. C.; Thummel, R. P.; Turro, C. *Journal of Inorganic Biochemistry* **2013**, *121*, 77–87.

[11] Kalyanasundara, K. *Photochemistry of Polypyridine and Porphyrin Complexes*, Academic Press, San Diego, 1992. 28

[12] Kobayashi, N.; Ishizaki, T.; Ishii, K.; Konami, H. *J. Am. Chem. Soc*. 121 (**1999**) 9096 – 9110. 29

[13] Ford, P. C. *Coord. Chem. Rev.* 44 (**1982**) 61 – 82. 30

[14] Tfouni, E. *Coord. Chem. Rev*. 196 (**2000**) 231 – 305. 31

[15] Van Houten, J.; Watts, R. J. *Inorg. Chem*. 17 (**1978**) 588 – 593. 32

[16] Durante, V.A.; Ford, P. C. *Inorg. Chem.* **1978** *18*, 3381 – 3385. 33

[17] Knoll, J. D.; Albani, B. A.; Turro, C. *Accounts of Chemical Research* **2015**, *48* (8), 2280–2287.

[18] Respondek, T.; Sharma, R.; Herroon, M. K.; Garner, R. N.; Knoll, J. D.; Cueny, E.; Turro, C.; Podgorski, I.; Kodanko, J. J. *ChemMedChem* **2014**, *9* (6), 1306–1315.

[19] Respondek, T.; Garner, R. N.; Herroon, M. K.; Podgorski, I.; Turro, C.; Kodanko, J. J. *Journal of the American Chemical Society* **2011**, *133* (43), 17164–17167.

[20] Foxon, S. P.; Green, C.; Walker, M. G.; Wragg, A.; Adams, H.; Weinstein, J. A.; Parker, S. C.; Meijer, A. J. H. M.; Thomas, J. A. *Inorganic Chemistry* **2012**, *51* (1), 463–471.

[21] Sullivan, B. P.; Calvert, J. M.; Meyer T. J. *Inorganic Chemistry* **1980**, *19*, 1404 – 1407.

[22] Takeuchi, K. J.; Thompson, M. S.; Pipes, D. W.; Meyer, T. J. *Inorganic Chemistry* **1984**, *23* (13), 1845–1851.

[23] Hecker, C. R.; Fanwick, P. E.; McMillin, D. R. *Inorganic Chemistry* **1991**, *30*, 659 – 666.

[24] Löser, R.; Schilling, K.; Dimmig, E.; Gütschow, M. *Journal of Medicinal Chemistry* **2005**, *48* (24), 7688–7707.

[25] Demas, J. N.; Harris, E. W.; McBride, R. P. *Journal of the American Chemical Society* **1977**, *99* (11), 3547–3551.

[26] Murov, S. L.; Carmichael, I.; Hug, G. L. *Handbook of Photochemistry, Second Edition*; CRC Press, 1993.

[27] Knoll, J. D.; Albani, B. A.; Turro, C. *Chem. Commun.* **2015**, *51* (42), 8777–8780.